The roofing system of the tholos of Athena Pronaia in Delphi: archaeological hypotheses and structural suggestions

D. Aita [1] , V. Beatini [2], E. Garavaglia [1], V. Paris [3], A. Pizzigoni [4], L. Sgambi [5]

[1] Politecnico di Milano, Department of Civil and Environmental Engineering (DICA), 20133 Milano, Italy (danila.aita, elsa.garavaglia)@polimi.it

[2] Aarhus University, Department of Civil and Architectural Engineering, 8000 Aarhus C., Denmark - valentina.beatini@cae.au.dk (corresponding author)

[3] University of Bergamo, Dipartimento di Ingegneria e Scienze Applicate, 24044 Dalmine (BG), Italy - vittorio.paris@unibg.it

[4] University of Bergamo, Italy (former professor) - attilio.pizzigoni@gmail.com

[5] Université catholique de Louvain, Louvain research Institut for Landscape, Architecture, Built Environment, 7500 Tournai, Belgium - luca.sgambi@uclouvain.be

The roofing system of the tholos of Athena Pronaia in Delphi: archaeological hypotheses and structural suggestions

This study aims to provide an integrated understanding of archaeological findings by evaluating reconstruction hypotheses from a technological and structural perspective, focusing on the Tholos of Athena Pronaia in Delphi, a prime example of 4th and 3rd-century BC Greek architecture.
Archeological research primarily focuses on proportional rules and decorative aspects. The original roof configuration remains uncertain despite its architectural significance and characteristic interlocking marble tiles. The investigation of structural problems is crucial for selecting the most feasible reconstructions and formulating hypotheses on materials, dimensions of structural elements, and how connections between elements were constructed.
Due to the many reconstruction uncertainties, a reverse design approach was employed, utilizing schematic technological sections based on the known structural and technical knowledge of the time to ensure consistency between archaeological images and potential underlying structural diagrams.
Variables were considered for uncertain dimensions, and the structure's safety was analyzed in terms of material strength and stability. This highlighted not only unsafe solutions but also potential novelties in structural conceptions. This contribution serves as a starting point for research, placing structural mechanics at the service of archaeology with a focus on the tholos roof system.

Keywords: Ancient timber structures; Tholos of Delphi; archaic trusses; interlocking blocks; structural archaeology; stone roof tiles, Marmaria.

1. Introduction

1.2 The tholos of Athena Pronaia

The tholos of Athena Pronaia in Delphi dates to the first decades of the 4th century BC. Ruined, seen within its location, still presents a powerful, evocative image (Pizzigoni, Attilio 2023), Figure 1. Built after 363 BCE, this tholos was praised as an architectural masterpiece due to the intricate match between its construction, structure, and decoration (Bousquet 1993a). In his book VII, Vitruvius mentioned that the architect,

Theodoros of Phokaia, wrote a treatise called 'De Symmetriis,' which is now lost but could have offered insights into the design's sophistication.

New The architectural typology of the tholos temple is a round building, characterized by a cella, sometimes a peristyle, and a podium (George and Liddell 1968). Today, the study of ancient buildings offers insights into locally sourced construction methods and inspires sustainable innovation in building (Guillaud 2014). Additionally, the tholos typology stands as a significant example of the tectonic approach, where each architectural element also serves as a vital structural component (Heinzl, Beatini, and Kirkegaard 2020). This approach emphasizes both structural integrity and aesthetic harmony, ultimately resulting in an efficiency solution that minimizes material waste.

Whether originally constructed in wood, like the rectangular temples, or derived from beehive tombs with corbelled domes, remarkable examples such as the tholos of Epidaurus, dating back to the 3rd century BCE, featured columns and roofing tiles made of stone. The Choragic Monument of Lysicrates, also from the 3rd century BCE, is the only tholos with its original roof intact, a small stone roof with a diameter of 2.8 meters. Notably, the use of heavy, brittle stone tiles in these constructions sets them apart from circular structures in other ancient cultures, which often employed more flexible and lightweight roofing materials. It is evident that these tholos structures required a substantially stiff structure to support the weight with little displacements, or the stone tiles shall have been robust enough to redistribute internal forces in case of local failure.

After Laurent rediscovered the tholos in 1838, a number of scholars organized excavations on the site; among them, Foucart, Homolle, Charbonneaux and Gottlob (Aita et al. 2023). The survey has been a lengthy process, hindered by technical limitations in survey methodologies available at the time and economic resources.

Extensive corrections and integrations are documented (Kyriakidis 2010). Given the prominence of the building, one of the first photogrammetric studies (Tokmakidis et al. 1998) used some of its elements as a case study. In 1936 three of the exterior columns and surmounting frieze were reassembled. However, during the restoration, it was used one block less for each column than what successive excavations demonstrated to be correct.

The region is known for its seismic activity and landslides. By the time of Pausanias' 'Description of Greece' in the 2nd century CE, the tholos was already in ruins, though the exact causes of its failure remain unknown. Sharp cutting stones on-site (Huber et al. 2022) suggest that once the structure failed, the blocks were likely further broken down for use in other constructions (Charbonneaux 1955). Numerous findings are preserved in the Delphi Archaeological Museum and on-site, but determining their original shapes and functions can be challenging. Now, the tholos is part of a large archaeological site. The École Française d'Athènes completed an impressive archiving campaign in 2021 that provided an updated status (Huber et al. 2022). Accordingly, there are at least 421 blocks belonging to the building, many of which have yet to be analyzed. The lack of constructed references and the potential use of sophisticated symmetry operations add to this difficulty in establishing the original form.

This research, beginning with the elements whose presence and position archaeologists have agreed upon, aims at translating the reconstruction hypotheses developed so far into possible structural schemes. These schemes serve as a basis for assessing the underlying structural system and to reason on technological aspects. In doing so, this approach clarifies which solutions may have been feasible and pinpoints

aspects that may require further investigation, helping to guide the selection of targets for potential future survey campaigns.

1.2. The composing architectural elements

From the ruins of the tholos, archaeologists have agreed on the plan, which is illustrated in Figure 2a. The measures adhere to the drawings developed by Bousquet (1993), who remarked how a correct dimensioning of the tholos shall account for the original units of measure, the dactyl, and be based on proportional rules. Not merely for their aesthetic value, geometrical proportions were used in ancient Greece to position elements on (Osthues 2014). Bousquet further demonstrated how the positioning and sizing of all elements of the stylobate, the columns, and the cell up to the arrangement of the paving stones can be traced by drawing nested truncated pentagons. Figure 3 illustrates the traces of pentagons that may have been used to size and position the elements in plan. Bosquet eventually searched for similar proportions in the elevation but working on the first survey by Gottlob (1925), certain assumptions eventually turned out to be inaccurate. The elevation and sections present many uncertainties: Figure 2b illustrates the elements whose location and shape has been agreed upon.

Below the stylobate, seven layers of cut stone have been found (Gottlob, K. 1925). Over the stylobate, the tholos comprises a peristyle of twenty Doric columns and capitals of combined height equal to 592 cm and a circular cell of height at least 509 cm (Kirk 1968), if composed only by standard blocks, and up to 668 cm (Bousquet 1993), if designed to match proportional rules. The uncertain dimensions are indicated with a question mark in the picture. The height of the cella is significant as regards the possibility to provide intermediate support to the roof above. Depicted in the section drawing, some blocks were recently analyzed (Huber et al. 2022) that could be the

toichobates and orthostates of the wall, typical elements of the base of the wall in classic Greek architecture: this may support the hypothesis of a high wall.

Either in contact or slightly apart from the wall of the cella, there were Corinthian columns, of which fragments of one or more capitals remains. Whereas the number of these columns has been debated, the most recent on-site observations tend to confirm (Bommelaer 2015) that they shall have been nine and in contact with the wall. It is known neither their height, nor if they were resting below other elements. Uncertainties concern all the elements of the entablature, the number of acroteria and the shape of roof. Albeit the height of the frieze is known, many of its triglyph blocks currently lie on the ground and appear to have similar fracture lines (Figure 4), which may provide insight into the failure mode of the roof and its structure thereof. The entablature of Greek monuments and temples typically presents careful carving that may have favored alignment of elements and stability also during construction (Manidaki 2019). An element of the geison was measured by Gottlob in the first official archeological survey of the tholos (Gottlob, K. 1925), Figure 5a. Accordingly, it spans halfway two columns, and its upper part is partially flat to the inside of the tholos and sloping to the outside with an angle $\alpha \approx 11.5^{\circ}$ to the horizontal. It is here supposed that its flat part may form the base for an acroterium resting on the columns. Meanwhile, other geison blocks that belong to the same temple have a different profile and slope, Figure 5b. The internal side of the geison is typically grooved, as exemplified in Figure 5c, which depicts the typical geison block of the Choragic monument of Nikias in Athens. The carving was possibly made to host timber elements. In the case at hand, in the absence of a relief, it can be ascertained neither its size nor if it repeats the same throughout the different blocks.

Moving upward, the sima (gutter) has long been debated over by archeologists. Two sima elements have been found, Figure 6, which differ in size and decoration. The bigger one is well wear; its sides are flat cut, it has a length $l \approx$ 140 cm (half the span

between the columns) and it tapers in plan to match a circle of external radius $r \approx 704$ cm, which suits the Doric peristyle. The smaller one is contemporary, but it is less degraded by running water. Its sides seem to be cut inclined to the horizontal, and the corresponding radius seems to be in between the one of the cella and the peristyle. Since the finds relating to the smallest sima are made up of small pieces, the data are difficult to ascertain exactly. Finally, some broken elements have been found, that present a geometrical pattern of carving. In line with the validated reconstruction hypotheses of rectangular temples, (Gottlob 1925) supposed that they may have been part of a coffered ceiling covering the peristyle. These elements are depicted in red in Figure 2 remarking that the hypothesis so far has been neither further investigated nor proved. Concerning the roof, fragments and three larger broken elements have been found, the latest ones reported in Figure 7. They all appear to belong to a set of very large stone tiles. It is not clear if the tiles were all equal, but Roux, the archaeologist that first studied them (Roux 1952), reported that the tiles are of a very curious type. They are antecedent, similar and more complex than the so called Corinthian ceramic tiles (Sapirstein 2009), imbrexes, that eventually developed. The tiles shall have been longer than 75 cm and have variable, up to 15 cm, thickness. Carefully carved, they have recesses and protuberances (Figure 7). None of these tiles are completely intact and only a couple can help identify how they could have been arranged. Archaeologists have interpreted them as imbrex and proposed also complex roofing patterns to accommodate them. Fragments of statues have also been found (Bommelaer 2015), whose location, size and weight have not been agreed upon. In various reconstructions, it is supposed that an acroterium rested on top of the roof, its height ranging from 1 m (Pomtow 1912) to 1.7 m (Bommelaer 2015), 2.6 m (Bommelaer 2015) and 3 m (Hoepfner 2000a). Its weight, calculated from the reconstruction drawings, could have

ranged from 3.7 KN to 99.5 KN. Again according to the reconstruction drawings, the possible acroteria resting on the columns, depicted in (Bommelaer 2015), could have had an height between 1.5 m to 2 m and weight between 3.5 KN to 4.5 KN. Given the above, the very shape of the roof is uncertain. Various reconstruction hypotheses have been formulated that highlight one or another aspect of the unique building. Recently, (Pizzigoni, Paris, and Beatini 2022a) took over the suggestion of Bousquet and proposed to extend the role of proportions to the third dimension employing an icosahedron, a figure that Euclide derives from two interlacing pentagon. They suggested that the dimensions of the tholos in 3D could be regulated by a vertically oriented icosahedron, with its upper and lower pentagons matching the size of the pentagon inscribed in the circumference of the stylobate, Figure 8.

All the solutions that have been studied by archaeologists over the years assume a wooden roof and are analyzed here. To the best of the authors' knowledge, these are the contributions of Laroche (1992), Roux (1952) and, from the same survey campaign, his student Kirk (1968), Pomtow (1912), Hoepfner (2000), and Bommelier with Laroche (Bommelaer 2015). These design hypotheses are reviewed not in chronological order but starting from the structurally simplest ones, so that the knowledge deduced from the analyzes of a solution can be reported if appropriate in the analysis of the more complex solution. Recently, contributions from architectural engineering started investigating the possibility that complex stone tiles could be employed in a self-supporting dome (Pizzigoni, Beatini, and Paris 2022b; Aita et al. 2023). Whereas that study is ongoing, in (Pizzigoni, Paris, and Beatini 2022b) it was demonstrated that a series of five stone tiles of this type could span between supports likewise jack arches without underlying sheathing. This result is considered when developing structural systems.

2. Material and method

Carrying out a structural analysis of archaeological hypotheses is not a univocally defined operation on a methodological level. Structural checks in the modern sense were absent in Ancient Greece; structural mechanics was not yet developed, although the lever principle as well as the principle of virtual works/virtual powers were known or intuited (Benvenuto 1981; Sinopoli 2015). Examining the structure from the point of view of the theoretical knowledge of mechanics and geometry then available would be an extremely challenging research topic, which could clearly bring out the relationship between architectural and structural conceptions in antiquity. A similar objective was pursued in (Sinopoli and Aita 2022), where the static behaviour of the Diana Dome of Baia is analysed in the light of the mathematical knowledge available at the time.

As already mentioned in the Introduction, the research proposed here aims to investigate the structural feasibility of the different roofing hypotheses proposed by the previously mentioned archaeologists (see Section 1.2). Extending the analyses conducted in (Sinopoli and Aita 2022; Aita et al. 2023) attention is here focused on gravitational loads, evaluating whether the tholos reconstructions, in particular their design, their geometry as well as the properties of the hypothesized materials, are acceptable from a structural point of view.

A difficulty emerges in this operation. As mentioned above, the concept of kinematics was certainly present in Greek mechanics from a theoretical point of view; for this reason, the solutions proposed by the architects may have been conceived with the aim of avoiding collapse mechanisms rather than paying attention to the strength of the materials, a concept that emerged from Galileo onwards (Benvenuto 1981). We are aware that the tholos project did not include any structural analysis in the modern sense by the ancient architects, who designed through processes that also involved trial and

error. At the same time, to verify whether a reconstructive hypothesis proposed by archaeologists is compatible with stability requirements, it is necessary to make use of modern structural mechanics. Feasibility from a structural point of view focuses on the static admissibility of the solutions, on verifying that they are not subject to collapse or excessive deformability.

Having therefore clarified the field of investigation of this contribution, in awareness of the problems described above, the analyses presented in this Section will refer to some standards present in Eurocode 5. This reference is chosen keeping in mind that the current standards could be more restrictive than the rules of good construction in force at the time of the construction of the monument.

The hypotheses developed by archaeologists typically focus on form and decoration. Therefore, they have been expressed in front views, integrated sometimes with details aimed to demonstrate the likeliness of the reconstruction in relationship with the findings. To move from form to construction, here possible conformal technical sections are proposed, according to which structural models are investigated. Of course, nowadays alternative structural systems can be successfully employed to solve the task. Here, reference is made to the construction techniques known to be available at the time, as well as to the size limits imposed by the findings.

Table 1 reports the characteristic strengths of the materials used in the analyses. For the wood-based reconstruction hypotheses, it is reasonable to assume that fir could have been employed: in (Lamouille 2020), it is attested that fir was ordered in connection with the construction of a Delphi temple, presumably the temple of Apollo. In (Klein 1998), it is further documented that fir and pine were common wood species used in classic Greece for the construction of vessels and buildings. The material proprieties are set according to EN 338-2016, assuming a conifer wood species in class

C18. The material properties of marble can vary according to the specimens size and testing method as much as between 58.5 MPa-116 MPa (Papantonopoulos 2006). In (Koroneos, Tassojannopoulos, and Diamantopoulou 1980), medium strength values of pentelic marble from two Greek quarries are in the order of 46 MPa. The values of the compression strength and the other stone material parameters are taken from this source. Concerning the frictional interface between stone and wood, the Forest Products Laboratory at the United States Department of Agriculture Forest Service (2010) suggests considering coefficients of kinetic friction for smooth, dry wood against hard, smooth surfaces within the range from 0.5 to 0.7 for intermediate moisture content. Acknowledging that the definition of the frictional interface between stone and wood would require experimental testing with the actual materials, here a value of static friction coefficient $\mu = 0.7$ is used.

Table 1 Material proprieties of fir and marble used in the analyses.

Conifer wood		
Specific weigth	γ_w	4.50 kN/m^3
Mean modulus of elasticity parallel in bending	$E_{m,0,mean}$	9000 MPa
5 percentile modulus of elasticity parallel bending	$E_{m,0,k}$	6000 MPa
Mean shear modulus	G_{mean}	560 MPa
Characteristic bending strength	$f_{m,k}$	18 MPa
Characteristic compressive strength parallel to the grain	$f_{c,0,k}$	18 MPa
Characteristic compressive strength perpendicular to the grain	$f_{c,90,k}$	2.2 MPa
Characteristic tensile strength parallel to the grain	$f_{t,0,k}$	11 MPa
Characteristic tensile strength perpendicular to the grain	$f_{t,90,k}$	4 MPa

Characteristic shear strength	$f_{v,k}$	3.4 MPa
Pentelic marble		
Specific weight	γ_s	27 kN/m^3(Papantonopoulos 2006)
Characteristic compressive strength	$f_{c,k}$	46 MPa (Koroneos, Tassojannopoulos, and Diamantopoulou 1980)
Characteristic bending strength	$f_{m,k}$	18.5 MPa (Koroneos, Tassojannopoulos, and Diamantopoulou 1980)
Modulus of elasticity	E	1000 $f_{c,k}$
Shear modulus	G	0.4 E
Interface marble - wood		
Friction coefficient	μ	0.7

Given the inherent uncertainties surrounding materials, geometry, and boundary conditions, the objective is to ascertain whether various archaeological hypotheses are reasonable within the framework of modern regulations, and, if so, to provide rough dimensions of the elements, that could possibly be verified in future archeological campaigns. It is supposed at first approximation that purlins were set in place if necessary to avoid torsional movement. Due to the axial-symmetry, the structure is evaluated in 2D. Similarly, when sizing the timber elements, sturdy cross sections having a ratio b / h > 0.75 are assumed and local instabilities are disregarded.

Stress components are plotted alongside the limit design values established by the Ultimate Limit State of Eurocode 5 (European Committee for Standardization 1995). It shall be noted that such values are meant to describe the structure at risk of failure and are reported here to help preliminary judging the safety of the structure. The analyses verify firstly if the roof's structural elements can withstand the stress due to bending, shear actions, the stress due to the copresence of bending and axial actions, as

well as deflection. If the roof's structural integrity is confirmed as safe, subsequent analyses focus on the vertical components of the structural system, such as walls and columns, and their interaction with the roof. Concerning the vertical elements, dry, thick stone elements like those used in antiquity are nowadays not common, and there is a well-known lack of standardized analyses procedure (Beatini, Royer Carfagni, and Tasora 2019). The Eurocode, for example, does not deal with dry stone. Here, the analyses report the compression stress on the wall and columns versus the characteristic stress. More importantly, since wooden structures tend to generate small displacements at supports, the equilibrium versus overturning actions transmitted by the roof is addressed according to the specificity of the proposed structural system.

The assumed permanent load is the sum of the weight of the documented stone elements and hypothetical wooden elements. Considering the broken tiles findings (Figure 7), the thickness of the stone roof is set constant and equal to $t_s = 15$ cm. As mentioned, the roof is unusually heavy. To better visualize the feasibility of the structure, loads other than the permanent ones have been disregarded. To account for uncertainties, the latter ones have been incremented by a partial factor $\gamma_G = 1.35$.

For wooden elements, the characteristic variable of strength f_{Rk}, listed in detail in Table 1, is reduced as by Eurocode 5 to the design value of strength f_{Rd}:

$$f_{Rd} = f_{Rk} \cdot k_{mod,per}/\gamma_m \tag{1}$$

where $\gamma_m = 1.3$ is a reduction factor accounting for material uncertainties, set here for solid timber, and $k_{mod,per} = 0.5$ is a strength modification factor accounting for humidity conditions and load durations. The latter variable is set here to represent Service Class 3 of Eurocode 5, the lowest one, which typically reads for large, solid

beams subjected to high humidity conditions due to their non-uniform drying process and / or outdoor working conditions. The preliminary assessments evaluate bending, compression, shear stress as well as deflection. These are compared to the threshold values derived from the Eurocode.

For the design shear stress τ_d, it has been evaluated whether:

$$\tau_d \leq f_{v,d} \cdot k_{cr} \tag{2a}$$

where $f_{v,d}$ is the design shear strength and k_{cr} is a reduction factor of deep timber sections to allow for drying splits. The design shear value $f_{v,d}$ is due by Eq. 1.

$$f_{v,d} \cdot k_{cr} = f_{v,k} \cdot \frac{k_{mod,per}}{\gamma_m} \cdot k_{cr} = 3.4 \cdot \frac{0.5}{1.3} \cdot 0.67 = 0.87 MPa \tag{2b}$$

Therefore, this leads to:

$$\tau_d \leq 0.87\ MPa. \tag{2c}$$

For the design bending stress $\sigma_{m,d}$, it has been evaluated whether:

$$\sigma_{m,d} \leq f_{m,d} \tag{3a}.$$

where $f_{m,d}$ is the design bending strength. By Eq, (1), $f_{m,d}$ has to be evaluated as:

$$f_{m,d} = f_{m,k} \cdot \frac{k_{mod,per}}{\gamma_m} = 18 \cdot \frac{0.5}{1.3} = 6.92 MPa \tag{3b}$$

which leads to

$$\sigma_{m,d} \leq 6.92\ MPa. \tag{3c}$$

The design shear action on the beam supports, $\sigma_{v,d}$, will be evaluated taking in account the compression stress $f_{c,90}$ perpendicular to the grain, as follow:

$$\sigma_{v,d} \leq f_{c,90} \cdot k_{c,90}, \tag{4a}$$

where $k_{c,90}$ is a modification factor to accepting an increase in strain at the failure condition for this state of stress. By Eq, (1), this leads to:

$$f_{c,90,d} \cdot k_{c,90} = f_{c,90,k} \cdot \frac{k_{mod,per}}{\gamma_m} \cdot k_{c,90} = 2.2 \cdot \frac{0.5}{1.3} \cdot 1 \quad = 0.85 \text{ MPa}, \qquad (4b)$$

And such it shall be:

$$\sigma_{v,d} \leq 0.85 \text{ MPa}. \qquad (4c)$$

The combined action of compression or tension parallel to the fibers and bending in the elements is evaluated respectively as:

$$\eta_1 = \left(\frac{\sigma_{c,0,d}}{f_{c,0,d}}\right)^2 + k_m \cdot \frac{\sigma_{m,y,d}}{f_{m,y,d}} \leq 1 \qquad (5a)$$

$$\eta_2 = \frac{\sigma_{t,0,d}}{f_{t,0,d}} + k_m \cdot \frac{\sigma_{m,y,d}}{f_{m,y,d}} \leq 1 \qquad (5b)$$

where k_m is a factor that accounts for the inhomogeneities of the material, equal to 0.7 for solid cross sections; $f_{c,0,d}$ is the design compression strength parallel to grain. By Eq, (1), it is

$$f_{c,0,d} = f_{c,0,k} \cdot \frac{k_{mod,per}}{\gamma_m} = 18 \cdot \frac{0.5}{1.3} \quad = 6.92\ MPa \qquad (5c)$$

$f_{t,0,d}$ is the design compression strength parallel to grain. By Eq, (1), it is

$$f_{t,0,d} = f_{t,0,k} \cdot \frac{k_{mod,per}}{\gamma_m} = 11 \cdot \frac{0.5}{1.3} \quad = 4.23\ MPa \qquad (5d)$$

For uniformity of nomenclature the design shear action on the beam supports $\sigma_{v,d}$ can be written like:

$$f_{c,90,d} = \sigma_{v,d} = f_{c,90,k} \cdot k_{c,90} = .85 \cdot 1 \quad = 0.85 \text{ MPa}. \qquad (5e)$$

Finally, $k_{c,90}$ is a modification factor to accepting an increase in strain at the failure condition depending on the amount of unloaded area, versus the risk of splitting and the degree of compressive deformation. Concerning the deflection limits, excessive deflection of a wooden substructure may have damaged the interlocking tiles to the point of causing unsafe load redistribution. Therefore, the maximum deflection is

plotted, and considerations are made according to the system of constraints present in each proposed structural scheme.

The above analyses allow one to preliminary size the elements, which, in turn, helps evaluating their technical feasibility. As visible in Figure 5c, the stone elements could have been grooved, possibly to fit connecting elements, yet there is currently no information on the sizes of the recesses. Here, it is assumed that they provide a bearing length of at least 12 cm and can host a beam of at least 20 cm. These values are increased in the analyses when found not sufficient. In such a way, the feasibility of certain dimensional values and structural systems thereof could possibly be further verified in future archaeological campaigns.

3. THE CASE STUDIES.

3.1 The open cella

The first analyzed hypothesis is the simplest one: a covered peristyle and an open cella. This solution was suggested by Laroche (Laroche, 1992) to justify the presence of the two sima. This proposal of reconstruction is controversial, as regards the compatibility with the archaeological finds (such as the tripartite tiles) and for architectural reasons (with reference to the high reputation that the tholos had at its time as an architectural wonder). However, its analysis helps filter the possible causes of the fracture of the frieze.

An illustration of the potential solution can be seen in Figure 9. There are a total of forty short rafters, matching the number of geison blocks, spanning from the geison up to the wall of the cella. To translate this system in a structural diagram, some hypotheses on the constraints should be considered. As regards the roofing system, a first analysis can be performed by assuming a hinge at the upper end (point C) and a

roller support with friction at the base (point D), as reported in Figure 10a. Each rafter transfers the load to the cella and the column. The area of influence for each rafter is shaded in yellow in Figure 9a. The corresponding load is indicated with $q_{s(\alpha)}$ in the diagram, whereas the self-weight of the rafter is indicated with $m_{r(\alpha)}g$.

Parametric analyses were performed by means of the software Grasshopper for Rhino, by assuming the slope angle α of the roof varying from $10°$ to $34°$ with $2'$ interval. This range covers the approximate value of $11.5°$, which matches both the slope of the planar surface of the geison reconstructed by (Gottlob, K. 1925) and the high slope required for the roof to fit the suggestion of a circumscribing icosahedron (according to (Pizzigoni, Beatini, and Paris 2022a). A first preliminary analysis of the roofing system is conducted by assuming zero friction coefficient at the end *D*. This assumption, although unrealistic, is in favour of safety for the roof considered separately from the vertical supports, while it allows for understanding its overall structural behaviour. The size of the timber rafters' cross section is chosen by considering the compatibility with the timber available at the time, as described in the previous Section, and is supposed to be b x h = 20 cm x 25 cm. Figure 11 illustrates the typical force diagrams: the shear force, the bending moment and the axial force as well the most critical cross sections of the rafters. The sign convention adopted for the stress resultants as well as for the corresponding diagrams are that reported in (Buccino et al. 2005), p. 68 and p. 70. Figure 12 presents the parametric results for the most stressed cross-sections and their locations. These results include the maximum design shear stress τ_d (a), the bearing compression stress at support, $\sigma_{c,90,d}$ (b), the maximum design bending stress $\sigma_{m,d}$ (c),

and the utilization due to combined compression and bending action (d), while varying the slope α. The bearing length of the rafters is assumed to be 12 cm, in line with the section drawings. Given the uncertainty about the usage and shape of notches, these are disregarded in the calculation. The maximum vertical deflection δ_y is reported in

Figure 13 and increases with increasing slope α. As one would anticipate, the elements of the roof are well-equipped to withstand the load, and deformation is effectively controlled.

When considering the roof-column (or roof-wall) system, a first check is carried out with reference to the stresses present in the vertical elements. With reference to Figure 10, the compressive stress on the column is

$$\sigma_{c,d_c} = \frac{2 \cdot V_{D(\alpha)} + m_c g + P}{A_c}, \qquad (6)$$

where $m_c g = 73.2\ kN$ is the self-weight, $2V_{D(\alpha)}$ is the sum of the forces transmitted by

the two rafters to the column, function of the slope angle, and $P = 72.6\ kN$ is the

tributary weight of the entablature, depicted in light blue on the plan, Figure 9a. The

area A_c has been calculated assuming an average diameter of the column $t_c = 75$ cm.

Similarly, the wall is subjected to a compressive stress per meter length equal to

$$\sigma_{c,d_w} = \left(\frac{40 \cdot V_{C(\alpha)}}{\pi \cdot 2 \cdot c} + m_{w(\alpha)} g \right) / t_w, \qquad (7)$$

where $40V_{C(\alpha)}$ is the sum of the forces transmitted by the forty rafters placed along the

entire perimeter of the cell, function of the slope angle α (assuming that the height of

the external colonnade is fixed, the height of the internal wall increases with the slope

of the roof), c = 4 m is the radius of the cell, $m_{w(\alpha)}g$ is the self-weight per meter related to the wall, and $t_w = 60$ cm is the thickness of the wall. These stresses are reported in Figure 14 and are largely within the average values reported in Section 2.

When considering the roof-columns system, however, the zero-friction hypothesis assumed regarding the connection between the roof system and the vertical elements is not in favor of safety. A second analysis is then performed assuming that the constraint at point *D* is a frictional roller. In this case a horizontal thrust could occur which could compromise the stability of the column. Among other possible analyses, an investigation was conducted by considering that the structure is in equilibrium and at the incipit of sliding failure (Figure 15); in this case, the horizontal displacement of the rafter is resisted by the full frictional capacity of the wood – stone interface. This has been calculated conservatively with reference to the overturning of the column, assuming the relatively high value of friction coefficient $\mu = 0.7$:

$$H_D = \mu \cdot V_D. \tag{8}$$

The displacement may overturn the column around its base point *O* in Figure 15a. The overturning moment $H_D \cdot h_c$ shall be resisted by the stabilizing moment M_{st} due to the vertical components of the load. Therefore, is verified whether

$$M_{st} = \left(m_{c(\alpha)}g + P\right) \cdot t_c/2 + V_D \cdot (t_c/2 + e) \geq H_D \cdot h_c, \tag{9}$$

where t_c is diameter of the column, $h_c = 5.92$ m is the height of the column, $e = 0.20$ cm is the set eccentricity of the rafter's action V_D. The resulting values of the overturning and resisting moments are reported in Figure 15b: according to the adopted

scheme, the risk of overturning increases with the slope since the horizontal force H_D increases at a faster rate than the stabilizing moment. From these analyses it can be confirmed that the reconstruction which proposes the peristyle covered by the sole rafters could be compatible with structural stability.

3.2 The frustoconical roof over rafters

In 1968, Kirk (1968) first proposed that the two sima may belong to two different tholoi; the first building, to which the small sima shall belong, was either interrupted during construction or failed shortly after. He concentrated his study on the last one, which would have contained only the larger sima. He noted that the tripartite tiles create an angle between their right and left wings of $\phi \approx 45°$, that is the inscribed angle of an octagon. On this basis, Kirk schematized the plan of the tholos as an octagonal roof, reproduced in Figure 16a. The scheme indicates a series of eight rafters spanning from the vertexes of the octagon to its center. Over the rafters, span secondary elements that carry the heavy tiles. The rafters interrupt toward the center, creating space for a possible acroterium. A tentative section of the solution to fit the reference plan is depicted in Figure 16b. Since the design assumes that there is a substructure between the rafters and the tiles, the latter are assumed to rest on the horizontal surface of the carved frieze, which offers a larger bearing length. The span of the rafter is set as $r = 6.45$ m. From a structural viewpoint, the first consequence of the design is that the eight rafters can only transmit the load to the twenty columns in an uneven way. Figure 17 represents half of the linear development of the perimeter of the tholos (see *s* in Fig. 16a) highlighting the position of the support columns and that of the punctual loads transmitted by the beams. In the absence of tensile strength between the blocks, which

could generate hoop forces acting in the horizontal plane, the blocks that make up the frieze would consequently be stressed in a non-uniform way, which could have affected the stability of the system both under gravitational and seismic actions. On the contrary, if hooping elements had been present, this problem would not have arisen, making this solution emerge as a structural system compatible with the hypothesis proposed in (12).

For as far as the roof is concerned, the structural diagram of the rafters' system is depicted in Figure 18.

The roof can undergo small displacements both horizontally and vertically, displacements typical of traditional wooden structures without modern metal fasteners. In the structural diagram, this is reproduced by assuming roller supports at the outer ends of the beams and inserting a roller support sliding along the axis of symmetry of the system, to guarantee the static determinacy of the system. Given the symmetry of the structural system and boundary conditions, this fictional support does not generate any reaction. Moreover, the inner connection between the beams is supposed to be rigid. Lacking inputs from Kirk, two cases are illustrated that differ in the presence of the central acroterium or its absence. The notation related to the latter case is marked with a prime in Figure 20. The acroterium is supposed to have a weight of 99.6 KN, the largest one among those mentioned in the Introduction, and its weight is equally shared by the rafters. The applied load corresponds to the one acting on the tributary area hatched in Figure 16a: these are the self-weight of the rafters, $m_t g$, the tributary weight of the stone elements q_s, and either the tributary weight of the acroterium, $q_a = \frac{Q_a}{b \cdot a}$, (Figure 18a) distributed along the length *a* in Figure 16b, or the corresponding weight q_c of the stones if the acroterium is absent, Figure 18b. Figure 19 illustrates the internal forces and moment diagrams. In both cases the loads are high for a self-standing solid wood

rafter. In the analyses, assuming for simplicity that the rafter has a squared cross section, its side length has been increased here from 20 cm to 60 cm, in 5 cm steps. Figure 20 reports the results for the most stressed cross sections and their location. The presence of the heavy acroterium does not result to be a discriminant factor for the safety of the system. The design stress values are higher than the ones set by Eurocode for almost all cross sections, and sometimes even higher than the corresponding characteristic strength. It can be deduced that the roof would fall under permanent loads, except in case a very large cross section is employed. Despite the large bearing length of 20 cm at support, the bearing force, $\sigma_{c,90,d}$, would also exceed the design strength.

Accordingly, Figure 20c, the deflection is plotted only for relatively large sizes of the cross section, for which at least the stress due to pure bending is within or around the characteristic value. It can still be observed, however, that obtaining eight rafters with such large cross sections in solid timber would have been difficult, or the design would imply that the wood section was layered. In (Aita et al. 2023), the possibility that a frustoconical octagonal dome made of load bearing stone tiles was investigated, yet it was failing due to instability. Both the octagonal shape and a simple beam spanning the entire tholos are therefore solutions difficult to support.

3.3 The double wooden roof

A proposal that is both technologically and structurally plausible suggests that the rafters rest on the cella. This concept was initially presented to the public in an elevation drawing published in 1912 by Pomtow (1912) (Figure 21). Criticisms from the archeological community concerning this solution deal with several aspects. Firstly, it appears unlikely that a meticulously decorated sima would be positioned in a way almost invisible to observers. Secondly, there are concerns about the varying levels of

wear on the two sima. Lastly and foremost, this proposal does not provide a satisfactory explanation for the presence of the tripartite tile (Kirk, 1968; Bommelaer 2015). Nevertheless, the underlying structural and technological systems introduce informative elements worth discussing.

The simplest structure derived from Figure 21 consists of 40 rafters spanning from the columns to the cella, along with 20 rafters covering the cella. Near the center, where the rafters would intersect, they are interrupted to provide support for the central acroterium (see Figure 21a). For the sake of simplicity, the weight of the acroterium distributed among the eight rafters is set to the average value Q_A = 37.2 kN /40 (see Section 1.2). The tributary area of one rafter is shaded in yellow in Figure 21. The loads due to the self-weight of the rafters, $m_{t,(\beta)}g$, and the stone tiles, $q_{s,(\beta)}$ vary with the slope angle β. The latter one reaches here a peak value of 6.26 kN/m at the supports.

The structural diagram is depicted in Figure 22. Since the structural system covering the peristyle is the same as the one analyzed in Section 3.1, just the roof over the cella is investigated, by varying the values of the slope angle β of the roof. Two friction rollers are assumed at the external ends (see point B), while at point A it is assumed a fictional roller support acting orthogonally to the axis of symmetry to assure the static determinacy. The inner connection between the two beams is supposed to be rigid. The analyses on the roof, considered separately from the vertical supports, are conducted by assuming zero friction coefficient in favour of safety. Here, it was necessary to increase the cross-section size of the rafter from b x h = 15 cm x 20 cm to b x h = 25 cm x 30 cm for all slope values. The typical internal forces and moment diagrams are illustrated in Figure 23. The analysis results are presented in Figures 24. The low stress value

compared to the design strength suggests that the roof structure would be strong enough. Additionally, the deflection (Figure 25), although considering only permanent actions, remains within the range of 2.5 cm to 3 cm, roughly 1/500 of the diameter of the cella. As for the roof covering only the peristyle, this static scheme confirms that, by keeping the plan of the tholos fixed, the stress on the critical section increases as the slope angle increases. Nevertheless, the system remains feasible.

To complete this preliminary study, the stability and stress of the wall are ascertained, Figure 26. The wall, despite being a continuous element, is interrupted by a large door, which affects its ability to exert hoop stress (Beatini, Royer-Carfagni, and Tasora 2018). Therefore, 1 m long element is considered isolated. The horizontal displacement of the central rafter at support B is counteracted by the presence of the outer rafter and by the frictional interface between stone and timber. Therefore, assuming as before that the wall is stable in a limit condition related to the friction constraints at the base of the roof, the resultant horizontal frictional reaction would be

$$(H_B - H_C) = \mu \cdot (V_B - V_C). \tag{10}$$

Such reaction could overturn the column around its base point *O* in the figure. The stabilizing moment M_{st} due to the vertical components of the load shall results:

$$M_{st} = \left(m_{W_{(\beta)}} \cdot g\right) \cdot t_c/2 + V_B \cdot (t_c/2 + e) + V_C \cdot (t_c/2 - e) \geq (H_B - H_C) \cdot h_w. \tag{11}$$

The height of the wall is $h_w = 10.2$ m, t_c is column diameter and $e = 0.15$ cm is the set eccentricity. The vertical reactions V_B and V_C are calculated per meter length of

the wall; $m_{w_{(\beta)}} \cdot g$ is self-weight per meter related to the wall. According to the results, Figure 26, the wall is stable, albeit the ratio between the stabilizing and the overturning moment is higher than in the case of the column. In fact, the same figure reports the overturning moment $H_B \cdot h_w$ that the cella would exert, if not counteracted by the rafters of the peristyle. Without that contribution, the stability of the wall would be at risk. It can be deduced that the possible coffered stone ceiling of the peristyle suggested by Gottlob (in red in Figure 2), may have been in place with a stabilizing function.

3.4 The double wooden roof with tripartite tiles.

In 2000, also introduced a system that proposed two roofs, visually appearing as if in a seamless continuation of each other. What makes this proposal particularly intriguing is its consideration of the tripartite tiles' shape. Hoepfner suggested that connecting the large rafters covering the cella would have been challenging. To address this, the architect might have employed a clever solution: he may have recessed every other rafter and inclined them toward the adjacent one in a symmetrical manner (see Figure 27a). By doing so, whereas the standard rafters would meet approximately at an angle of 18°, certain rafters could have potentially met at an angle of about 45°- 48°. The design of the tripartite tiles could have been orchestrated to conceal these connections. The archeologist also proposed that a central, groomed element could have connected the remaining 10 rafters together while serving as a base for the acroterium. Hoepfner's comprehensive text does not delve into the rationale behind the roof's slope, nor does it include a section of the entire structure. With the elevation drawing created by the archaeologist as a reference point, a provisional section is presented in Figure 27b. As in the previous case, the slope β of the roof of the cella is set to vary within the range of

10° to 34°. In Figure 27a, the tributary area of the most heavily loaded rafter is hatched in yellow, while the area of one of the rafters resting on the primary one is hatched in light blue. Additionally, Figure 28 illustrates the structural diagram of one of the primary rafters, alongside the rafter of the peristyle. Like the previous case, the load originating from the acroterium is conventionally set equal to 37.2 kN and distributed among the twenty rafters (Q_A = 37.2 /10 KN in the figure). Each couple of secondary rafters impose a load $2Q_r$ on the primary rafter, where Q_r ranges from 21.9 kN to 26.1 kN function of the slope β. Given the uncertainties concerning the exact position of the connection, this load has been assumed distributed along the span c = 0.6 m in Figure 27, such that it is $q_{r(\beta)} = \frac{2Q_{r(\beta)}}{c} = \frac{2Q_{r(\beta)}}{0.6}$. The loads due to the self-weight of the rafters, $m_{t(\beta)}g$, and the stone tiles, $q_{s(\beta)}$ are also considered. The typical diagrams of internal forces and moment are illustrated in Figure 29. In the analyses, it was necessary to further increase the size of the primary rafter to substantial dimensions, specifically b x h = 30 cm x 35 cm. However, as depicted in Figure 30, this rafter proves incapable of withstanding the added load. Both the maximum bending moment and the shear forces generate stresses that significantly exceed the limits recommended by the Eurocode. Meanwhile, to contain the bearing stress within acceptable limits, a bearing length of 20 cm has been assumed. Additionally, the deflection exceeds the thickness of the tiles, posing a clear risk of damage. It can be concluded that the arrangement of the tiles as shown in Figure 27 necessitates the presence of supports beneath the recessed joists or the implementation of an alternative structural system.

3.5. The rafter and joist roof

Excluding the hypothesis that the cella can be covered solely by rafter beams, one could investigate the employment of more sophisticated structural systems that do not affect the proposed organization of the roof tiles. Trusses could, of course, be considered for this purpose, but archaeologists and scholars specializing in ancient structures tend to agree that, if used at all, trusses were applied by the Greeks in ancient times, if any, in Sicily, but not on the mainland (Klein 1998). Meanwhile, in rectangular temples, rafters were connected through hangers to joists, which were supposedly resting on columns (Hodge 2010). In certain cases, it has also been suggested that no columns were present between the end supports; due to the deterioration of the timber elements, however, no definite proof could be established (Pierattini 2022). Here, it is hypothesized that such a system was adapted to the rounded temple. Accordingly (see Figure 31), all the rafters meet at the middle of the roof, as in the hypothesis discussed in Section 3.4, whereas the five most loaded rafters are also connected to five underlying joists by two hangers each, arranged symmetrically. The hangers are located under the overloaded part of the rafters.

From an architectural perspective, this solution would adhere to mathematical rules as the ones already suggested for the sizing of the stone elements of the tholos. Forty short rafters would cover the peristyle, twenty rafters would cover the cella; of these, ten would reach the top of the roof and 5 would create a rafter and joist system. If the composition of the plan (Bousquet 1993b) and possibly the elevation (Pizzigoni, Beatini, and Paris 2022a) are governed by hidden pentagons, a pentagon would be fully visible in the interior of the cella.

Concerning the structural aspects, the Archeologists have already agreed (Bommelaer 2015) that the inner (semi)columns of the cella were located close to the

wall. Therefore, no columns are set under the hangers. Without columns under the hangers, the system would not have been documented before and would have contained important novelties. Firstly, it leverages the tying action offered by the joists. It has been variously ascertained that the Greeks were well aware of employing the tying actions of ropes to connect timber arched elements in their military vessels (Brewster 1923) (Chatterton 1924). These ropes, called hypozomata (undergirding), were connecting the longitudinal ends of the hull, ensuring that it stayed in compression and watertight under adverse water conditions (Eliav and Helfman 2022) (Takako Niwa 2004). However, here the five lintels would have intersected at a point at midspan, Figure 31b. The connection detail could have been solved substituting the lintels with metal chains, yet, for what the authors could investigate, metal chains were not employed at that time; on the other hand, chains made of natural fibers were widely employed (Pierattini 2022), but they would have posed serious risks if a careful maintenance was not put in place. Alternative solutions may have been employed. Here, it is supposed that a floating element, for example an engraved trunk, could have connected the five lintels together. As illustrated in the plan, this circular element is set to have a diameter $2a$ = 80 cm and connects joists of cross section b x h = 25 cm x 25 cm. The hangers have cross section b x h = 15 cm x 15 cm. The rafters have cross section b x h = 25 cm x 30 cm as in the case at Section 3.3. Each joist and the central element superimpose for a length of 25 cm, where a splice and scarf joint could have been set. The structural diagram is illustrated in Figure 32a. Since the pentagonal geometry imposes that the five rafters are each on a different plane, each one is analyzed separately. As in the previous cases, roller supports are set at the connection with the wall of the cella. At their top, the constraint is assumed to be a slider acting orthogonally to the vertical axis of the tholos. A vertical roller connects the joists to the

central element. The connection hanger – joist (see point E" in Figure 32) is modelled as a hinge by considering this solution compatible with the construction techniques at the time. Consequently, for ensuring internal stability, the joint between the hanger and the rafter (point E) is modelled as rigid. As in the previous cases, the slope β of the roof is set as a design variable. As before, the considered loads are the self-weight of the wooden elements, $m_{s(\beta)}g$, the imposed load of the stone tiles, $q_{s(\beta)}$, the load of the acroterium, distributed the now ten rafters, $Q_a = \frac{37.2}{10 \cdot 2}$, and the load imposed by the secondary rafters, acting along the span c, $q_{r(\beta)} = \frac{2Q_{r(\beta)}}{c} = \frac{2Q_{r(\beta)}}{0.6}$. The diagrams of internal forces and moment are illustrated in Figure 33. The strength analyses are reported in Figure 34 and the deflection in Figure 35. It is interesting to observe that, for sloping angles β > 10°, the hanger is in tension. The system is always capable of carrying the loads within safe stress limits. Contrary to the previous cases, where a low slope of the roof was advantageous, here both the deflection and all the stresses except the bearing at support decrease up to a slope angle $\beta = 26°$; by further increasing the slope, β, the deflection and stresses in the rafter increase. Meanwhile, the bearing stress could have been diminished by increasing the bearing length, or by adding a prop resting on the columns. It shall be noted that the slope β does not necessarily coincide with the slope α of the outer roof (see Figure 31a). Therefore, a small slope for the roof covering the peristyle and a larger slope for the roof covering the cella would have been optimal. The solution would correspond to a roof with a sagging, variable profile.

Interestingly, this solution partially matches the most recent archeological reconstruction hypothesis proposed by Laroche (Bommelaer 2015): a sagging roof, in which the internal and external rafters oriented in plan along the roofs have two different slope angles, could be compatible with the small sima possibly tapered vertically.

It shall be noted, however, that in that solution the roof was based on diagonals of an octagon, which has already been found not feasible in Section 3.2.

4. CONCLUDING REMARKS AND FUTURE RESEARCH

Starting from some architectural and geometric elements deemed as certain as regards the composition of the tholos, the plausibility of the most accredited archaeological reconstructions has been investigated from a structural point of view. By studying the equilibrium and strength conditions of such structural systems, some critical issues have emerged regarding the different mechanical behavior depending on the type of constraints and loads acting on them. The research highlights that the hypotheses must be not only consistent with the findings, but also compatible with structural stability, construction techniques, and materials used at the time.

The choice of constraints in the structural schemes was performed in order to obtain statically determined (or indertermined) systems reasonably compatible with the construction techniques of the time, by studying both the stability of the roofing system and that of the system composed of the roof and the vertical supports (inner wall, columns).

The generally accepted hypothesis is that the load-bearing structure is made of wood and that the marble tiles are non-load-bearing elements of the roof. Aware of the interdisciplinarity of this research, this contribution questions some evidence that seems consolidated, but which nevertheless presents aspects to be explored in greater depth by

future archeological studies. Archeologists agreed on proportional rules governing the composition of the tholos, but these rules got lost in many of the evaluated elevations, or they would have led, as in the case of an octagonal roof, to a structurally unsafe structure. On the other hand, it is particularly interesting the concept of a sagging roof supported by a rafter and joist structure. This would have provided visitors with a unique opportunity to observe the underlying proportional principles in the physical arrangement of rafters and lintels. Notably, this structural design would have introduced novel elements by utilizing the knowledge available at the time in a groundbreaking manner and would have represented a significant advancement toward archaic trusses with props on the path set by the solutions of posts over columns employed in rectangular temples.

This research also highlights some aspects that could be explored in depth by future structural and technological research. As mentioned in the Introduction, the fragments of marble tripartite tiles play an important role in the reconstruction of the roofing system. In this study, it has been assumed based on (Pizzigoni, Paris, and Beatini 2022b) that the tiles can span between the rafters without underlying shifting. The same authors suggested that the tripartite tiles (without the addition of flat tiles) would form a self-supporting stone dome. Obviously, the behavior of a self-supporting stone roof would be very different from that of a wooden structure (Aita et al. 2023) On this aspect, further research developments include the in-depth study of various geometric solutions compatible with the stone finds and with the dome-like behavior of the roof. Furthermore, some details of the frieze will be studied, with particular emphasis on the failure plane of the frieze.

Finally, the examination of different structural solutions conducted in this work takes on an important significance as a starting point for future insights related to

another intriguing topic between structures and archaeology, i.e., the study of the tholos in the framework of the archaeoseismological approach (44), i.e., a methodology aimed at exploring ancient buildings as potential evidence of long-term seismicity since their construction.

Acknowledgements

The authors thank the École Française d'Athènes, and in particular Professor Didier Laroche, for sharing their knowledge and the open discussions, as well as the Archaeological Museum of Delphi for their availability and support.

References

Aita, D, V Beatini, E Garavaglia, V Paris, A Pizzigoni, and L Sgambi. 2023. "The Stone Roof of the Tholos of Athena Pronaia in Delphi. Structural Hyphoteses Starting from Fragments of Marble Tiles." The International Archives of the Photogrammetry, Remote Sensing and Spatial Information Sciences 48: 59–66.

Beatini, Valentina, Gianni Royer Carfagni, and Alessandro Tasora. 2019. "A Non-Smooth-Contact-Dynamics Analysis of Brunelleschi's Cupola: An Octagonal Vault or a Circular Dome?" Meccanica 54 (February). https://doi.org/10.1007/s11012-018-00934-9.

Beatini, Valentina, Gianni Royer-Carfagni, and Alessandro Tasora. 2018. "The Role of Frictional Contact of Constituent Blocks on the Stability of Masonry Domes." Proceedings of the Royal Society A: Mathematical, Physical and Engineering Sciences 474 (2209): 20170740.

Benvenuto, Edoardo. 1981. La Scienza Delle Costruzioni e Il Suo Sviluppo Storico. Sansoni. Florence.

Bommelaer, Jean-François. 2015. "Nouveautés Concernant l'architecture de La Tholos de Delphes." Comptes Rendus Des Séances de l'Académie Des Inscriptions et Belles-Lettres 159 (4): 1733–58.

Bousquet, Jean. 1993a. "La Tholos de Delphes et Les Mathématiques Préeuclidiennes." Bulletin de Correspondance Hellénique 117 (1): 285–313.

———. 1993b. "La Tholos de Delphes et Les Mathématiques Préeuclidiennes." Bulletin de Correspondance Hellénique 117 (1): 285–313.

Brewster, Frank. 1923. "The Υποζωματα of Ancient Ships." Harvard Studies in Classical Philology 34: 63–77. https://doi.org/10.2307/310674.

Buccino, Fernanda, Elsa Garavaglia, Elisa Guagenti, and Giorgio Novati. 2005. Statica: Fondamenti Di Meccanica Strutturale. McGraw Hill.

Charbonneaux, Jean. 1955. "Jean Marcadé, Recueil Des Signatures de Sculpteurs Grecs. Première Livraison. École Française d'Athènes, 1953." Revue Des Études Anciennes 57 (1): 172–74.

Chatterton, Edward Keble. 1924. Ships & Ways of Other Days. Lippincott.

Eliav, Joseph, and Nathan Helfman. 2022. “Lightweight Construction of an Athenian Trireme: A Feasibility Study.” International Journal of Nautical Archaeology 51 (1): 187–94. https://doi.org/10.1080/10572414.2022.2088216.
European Committee for Standardization. 1995. “Eurocode 5: Design of Timber Structures. EN 1995.” Brussels.
Forest Products Laboratory. United States Department of Agriculture Forest Service. 2010. “Wood Handbook, Wood as an Engineering Material.” General Technical Report FPL-GTR-190. Madison, WI: U.S.
George, Henry, and Scott Liddell. 1968. A Greek-English Lexicon. Clarendon.
Gottlob, K. 1925. “Relevés et Restaurations. (II. Topographie et Architecture. Le Sanctuaire d’Athéna Pronaia) 6, Paris, 1925.” In . Vol. 18. Fouilles de Delphes 2. Paris: De Boccard, G. http://ancientworldonline.blogspot.com/2014/03/open-access-monograph-seris-fouilles-de.html.
Guillaud, Hubert. 2014. VerSus: Lessons from Vernacular Heritage to Sustainable Architecture. Edited by Hubert Guillaud. Grenoble, France: CRAterre éditions. http://www.esg.pt/versus/images/pdf/versus_booklet.pdf.
H. R. Pomtow. 1912. “Die Grosse Tholos Zu Delphi Und Die Bestimmung Der Delphischen Rundbauten.” Klio, 1912.
Heinzl, Leo Gamborg, Valentina Beatini, and Poul Henning Kirkegaard. 2020. “A Retractable Roof Pavilion-Future and Precedent.” In Proceedings of IASS Annual Symposia, 2020:1–12. International Association for Shell and Spatial Structures (IASS).
Hodge, A Trevor. 2010. The Woodwork of Greek Roofs. Cambridge University Press.
Hoepfner, Wolfram. 2000a. “Zur Tholos in Delphi.” Archäologischer Anzeiger, 99–107.
———. 2000b. “Zur Tholos in Delphi.” Archäologischer Anzeiger, 99–107.
Huber, Sandrine, Didier Laroche, Manon Bublot, and Anne Jacquemin. 2022. “Delphes : les vestiges sur la terrasse de Marmaria, 2017-2021.” Bulletin archéologique des Écoles françaises à l’étranger, July. https://doi.org/10.4000/baefe.5278.
Kirk, Frode. 1968. Marmortag Paa Tholos i Delphi», Tilegnet Mogens Koch.
Klein, Nancy L. 1998. “Evidence for West Greek Influence on Mainland Greek Roof Construction and the Creation of the Truss in the Archaic Period.” Hesperia: The Journal of the American School of Classical Studies at Athens 67 (4): 335–74.
Koroneos, E. G., Al. Tassojannopoulos, and A. Diamantopoulou. 1980. “On the Mechanical and Physical Properties of Ten Hellenic Marbles.” Engineering Geology 16 (3): 263–90. https://doi.org/10.1016/0013-7952(80)90019-8.
Kyriakidis, Nicolas. 2010. “Erreurs à Delphes. La Tholos de Marmaria Au Fil Des Interprétations (ca 1840-1940).” Anabases. Traditions et Réceptions de l’Antiquité, no. 11: 149–63.
Lamouille, Stéphane. 2020. “The Wood Frame of the Temple of Apollon in the Accounts of Delphi: Techniques, Vocabulary and Building Work Chronology.” Bulletin de Correspondance Hellénique 144.
Laroche, Didier. 1992. “La Tholos de Delphes. Forme et Destination.” In Bommelaer, JF (Ed.) Delphes: Centenaire de La" Grande Fouille" Réalisée Par l’Ecole Française d’Athènes (1892-1903): Strasbourg, 6-9 novembre 1991.
Manidaki, Vasileia. 2019. “New Evidence for the Construction Phases of the Parthenon Peristyle: Anomalies at the Southwest Corner.” In New Directions and Paradigms for the Study of Greek Architecture, 39–55. Brill.

Osthues, Ernst-Wilhelm. 2014. “Bauwissen Im Antiken Griechenland.” In Wissensgeschichte Der Architektur. Vol. 2: Vom Alten Ägypten Bis Zum Antiken Rom, 127–261. Edition Open Access.

Papantonopoulos, C. 2006. “Spanning Intervals: Towards Understanding the Ancient Greek Optimization Procedure for the Design of Horizontal Beams.” Fracture and Failure of Natural Building Stones: Applications in the Restoration of Ancient Monuments, 257–68.

Pierattini, Alessandro, ed. 2022. “The Rise of Monumental Temples: Eighth to Mid-Seventh Centuries Bc.” In The Origins of Greek Temple Architecture, 56–178. Cambridge: Cambridge University Press. https://doi.org/10.1017/9781108583046.003.

Pizzigoni, Attilio. 2023. Osservando i Marmi Bianchi Della Tholos Di Delfi. Perché Sono Crollati i Templi Greci. Marinotti.

Pizzigoni, Attilio, Valentina Beatini, and Vittorio Paris. 2022. “The Stone Roof Marble Tholos Tiles in the Sanctuary of Athena Pronaia at Delphi. Stereotomy and Compression Resistant Forms in the Domed Roof Structures of Ancient Greece.” Structural 240 (art. n. 8): 1–30.

Pizzigoni, Attilio, Vittorio Paris, and Valentina Beatini. 2022. “Why Collapsed Ancient Hellenic Temples? The Case Study: Athena Pronaia Tholos at Delphi.” In , 2022:1–10. International Association for Shell and Spatial Structures (IASS).

Pomtow, H. R. 1912. “Die Grosse Tholos Zu Delphi Und Die Bestimmung Der Delphischen Rundbauten.” Klio, 1912.

Roux, Georges. 1952. “Le Toit de La Tholos de Marmaria et La Couverture Des Monuments Circulaires Grecs.” Bulletin de Correspondance Hellénique 76 (1): 442–83.

Sapirstein, Philip. 2009. “How the Corinthians Manufactured Their First Roof Tiles.” Hesperia, 195–229.

Sinopoli, Anna. 2015. “Il Problema Dell’equilibrio Da Aristotele a Varignon.” Il Problema Dell’equilibrio Da Aristotele a Varignon, 0–0.

Sinopoli, Anna, and Danila Aita. 2022. “The Dome of the Temple of Diana in Baiae: Opus Caementicium, Geometry and Mechanics.” International Journal of Architectural Heritage 16 (8): 1152–83.

Takako Niwa. 2004. “About the essential equipment for triremes ‘Hypozomata’ (In Japanese).” 日本航海学会論文集 111: 1–9.

Tokmakidis, Kostas, Juko Ito, Eiji Mamoto, and Fumiaki Mori. 1998. “Detail Surveys with Close-Range Photogrammetry in Archaeological Sites.” International Archives of Photogrammetry And Remote Sensing 32: 648–51.



Figure 1 The tholos of Athena Pronaia in Delphi, with the three columns and frieze elements set back up in 1925.

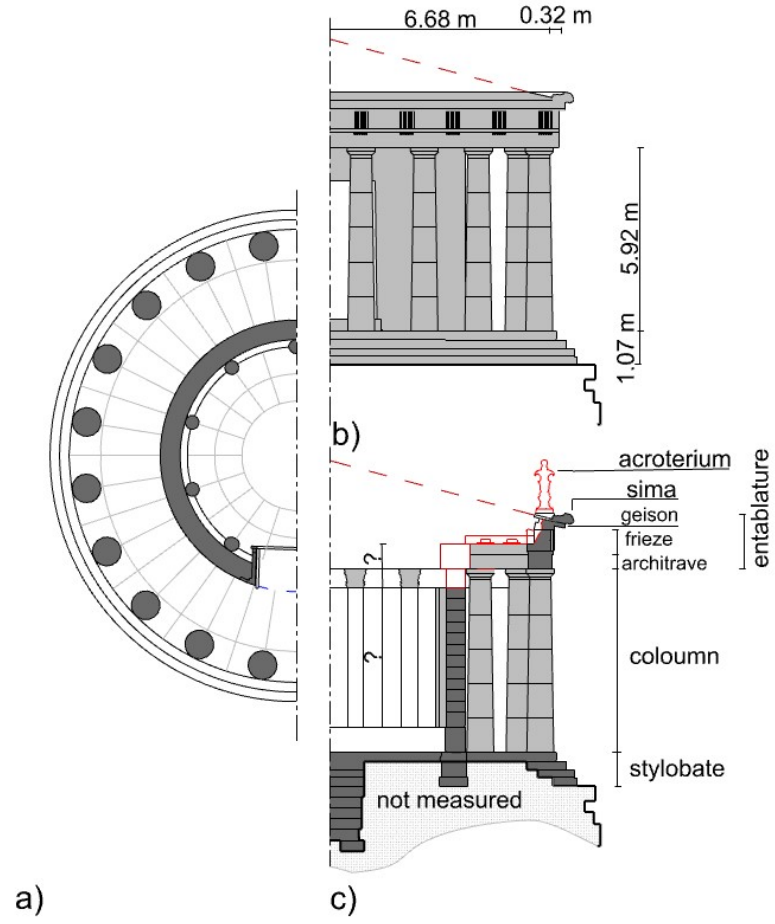


Figure 2 Plan (a), elevation (b), and section (c) of the tholos illustrating the elements whose location and size are agreed upon. In red, elements still to be confirmed.

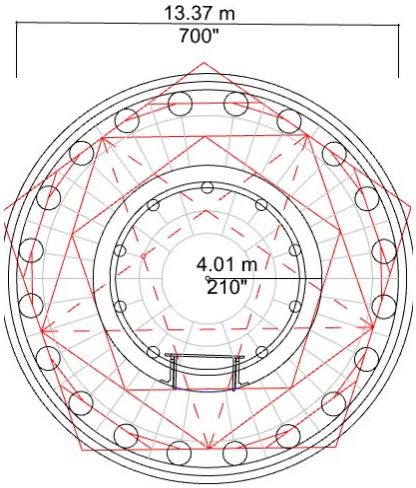


Figure 3 The pentagon polygons underlying the design of the plan of the tholos according to (11).



Figure 4 The frieze elements resting on site, which all appear to be broken along the same fracture plane. (Photo A. Pizzigoni).

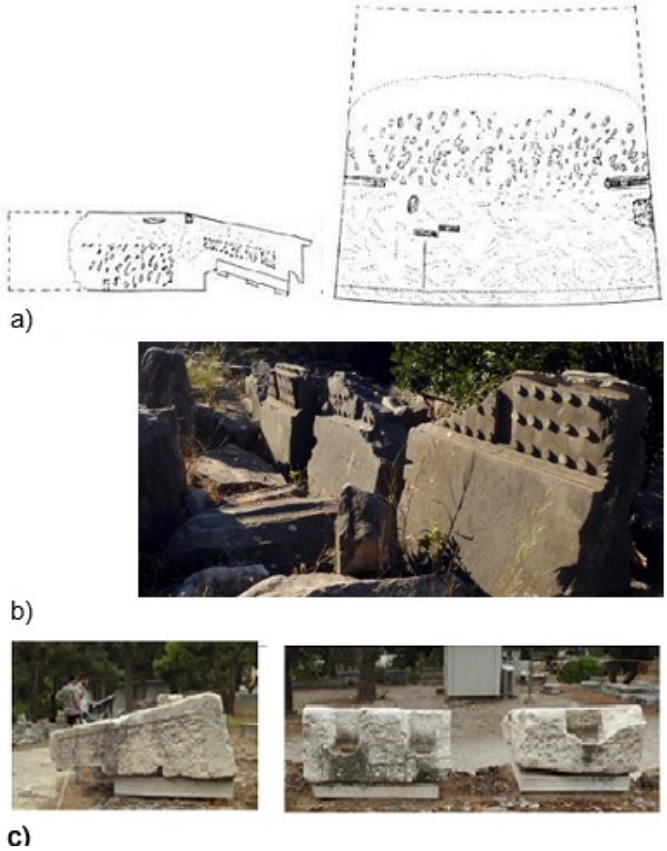


Figure 5 The side and top view of the gutter relieved by Gottlob, which has a flat part (a). The ones on site, which appear of constant slope (b). Side and back view of gutters in the Choragic monument of Nikias in Athens: note the engraving for connecting structural elements on the back side (c). (Photos A. Pizzigoni).

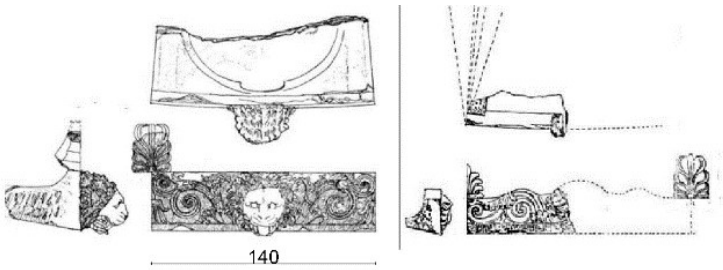


Figure 6 The big and the small sima fragments, from (12).

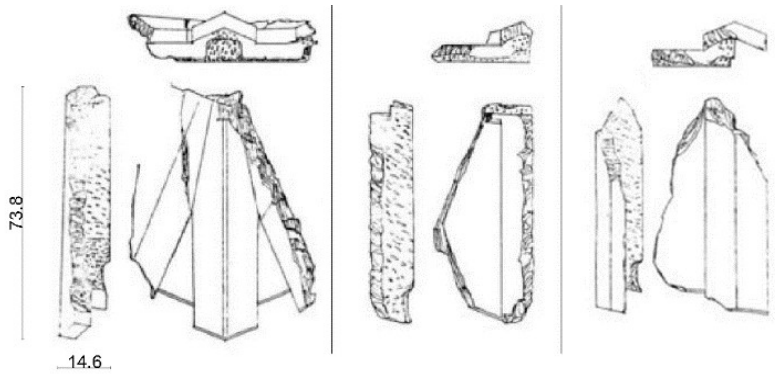


Figure 7 The biggest fragments of the stone tiles, adapted from (12).

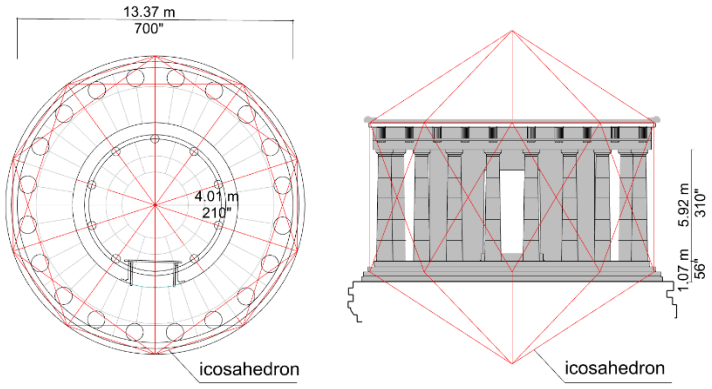


Figure 8 The icosahedron underlying the design of the tholos according to (4): in plan view (a), its profile creates two interlaced pentagons that may match the one proposed by Bousquet (11). In elevation (b), it may set the vertical limits of the tholos.

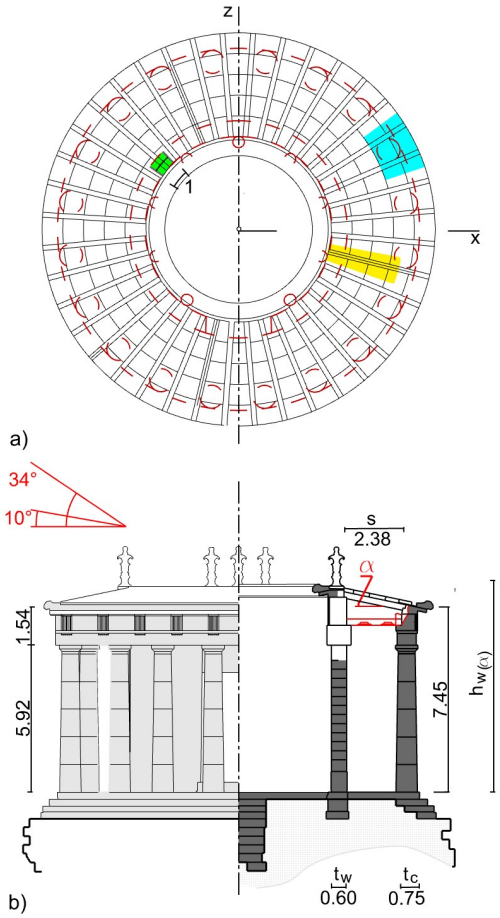


Figure 9 Plan (a) and elevation (b) of the tholos, hypothesizing that its roof covers only the peristyle.

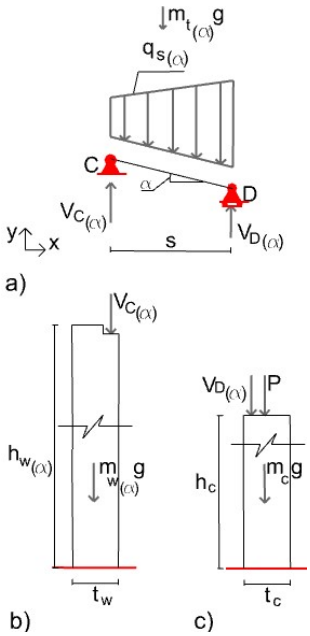


Figure 10 Free body diagram of the rafter (a), the wall (b) and the column (b), with indication of the applied loads.

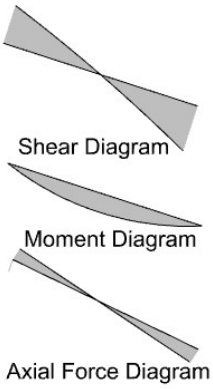


Figure 11 Typical force diagrams for the proposed structural scheme.

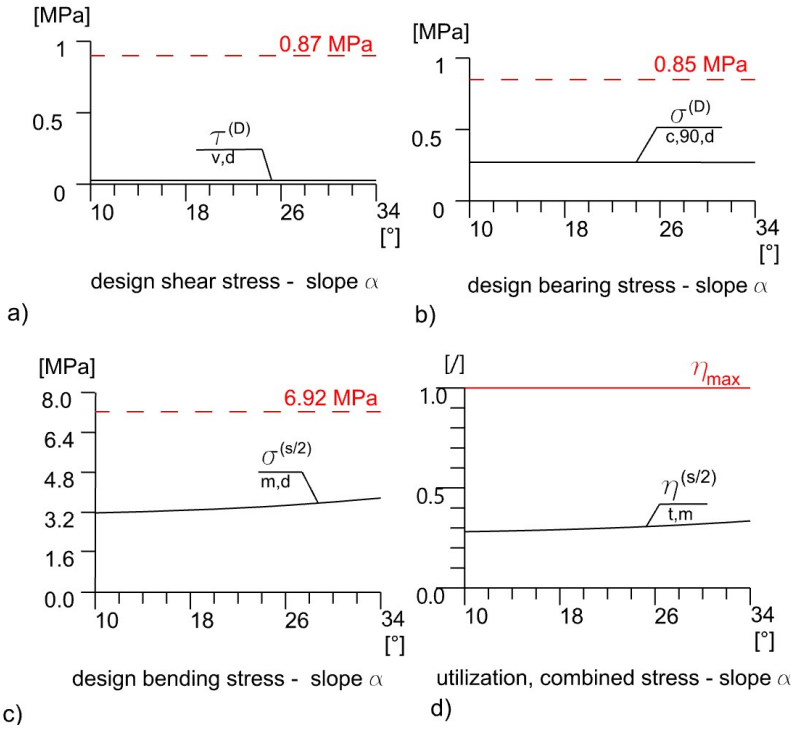


Figure 12 Stress analyses of the rafter covering the peristyle for variable slope of the roof. Design shear stress (a); design bearing stress (b); bending component of the stress (c); utilization due to combined compression and bending action (d).

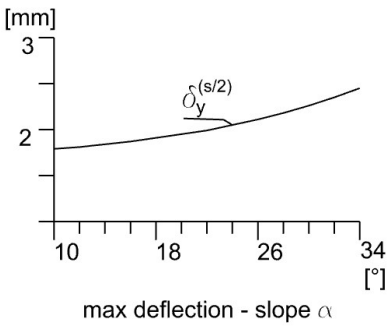


Figure 13 Maximum vertical deflection of the rafter for variable slope of the roof.

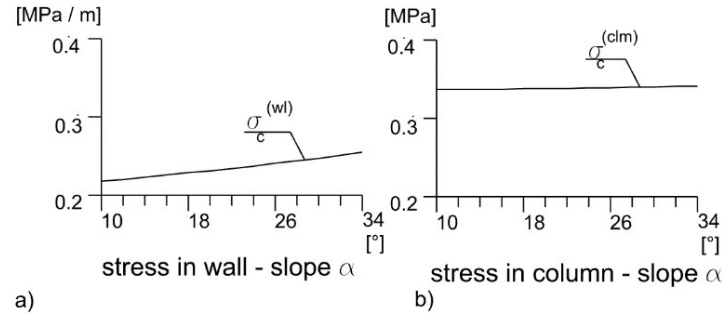


Figure 14 The low compression stress in the stone wall (a) and column (b) as a function of the variable slope angle α.

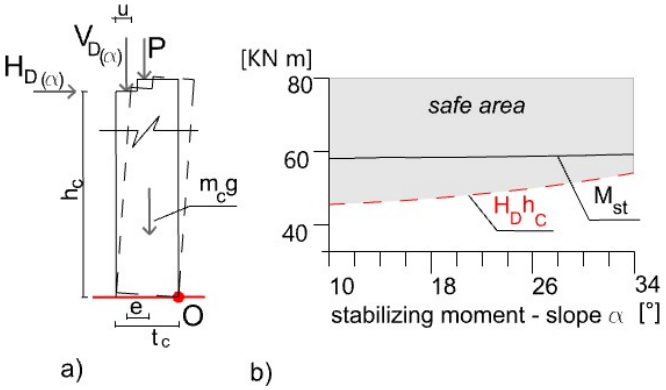


Figure 15 Free body diagram of the column under the horizontal action exerted by the rafter and the vertical loads (a). Stabilizing moment, M_{st}, plotted against the overturning moment.

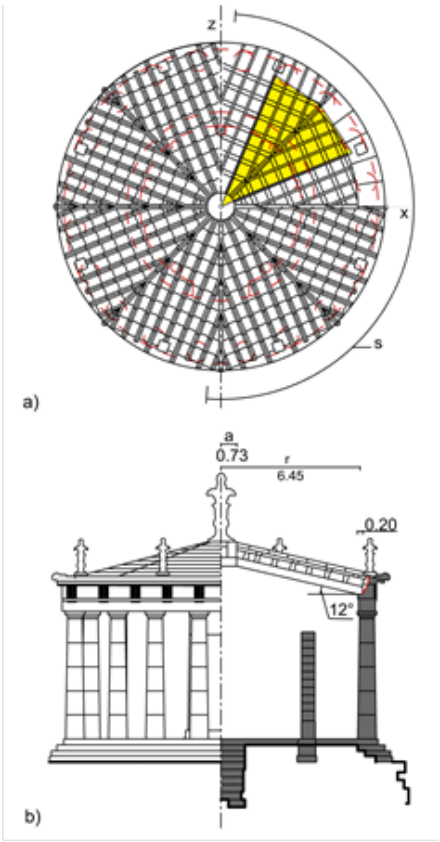


Figure 16 Plan view of the frustoconical roof proposed by Kirk. (a). Possible corresponding elevation and section (b).

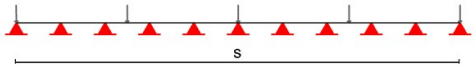


Figure 17 The eight rafters can transmit load to the ten columns only in an uneven way, as visualized for half the linear development of the perimeter of the tholos (curve s in Figure 16a).

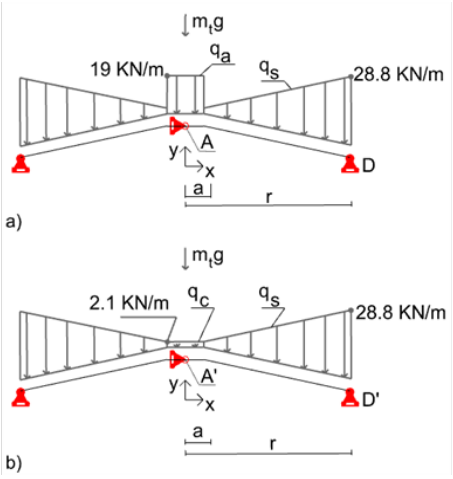


Figure 18 Structural diagrams of the octagonal roof: (a) considering a large acroterium at the top of the roof; (b) disregarding it.

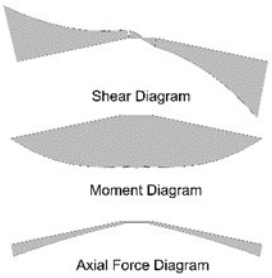


Figure 19 Typical internal forces and moment diagrams of the analyzed case.

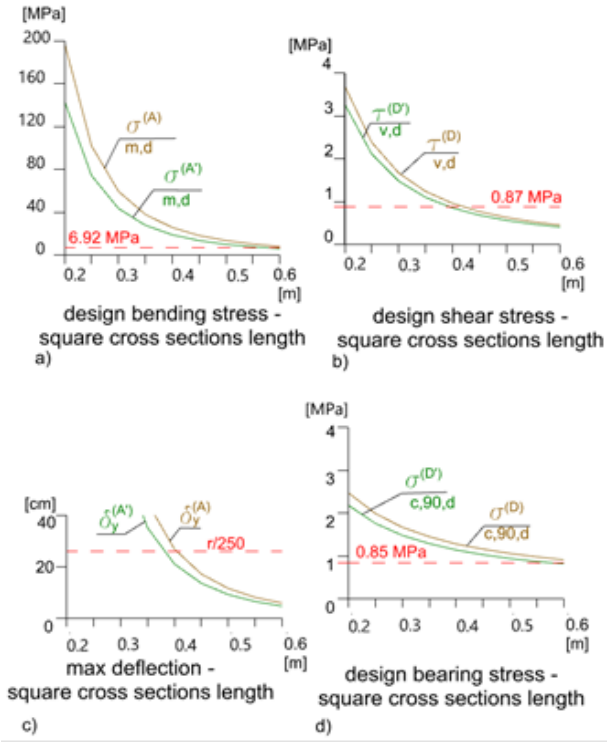


Figure 20 Structural analyses of the rafter for variable size of a squared cross section in the case of a roof with and without a large acroterium at the central top. The latter is marked with a prime. Bending component of the stress (a), design shear stress (b), maximum values of the deflection for concurrent compression and bending stress (c) and bearing stress at the supports (d).

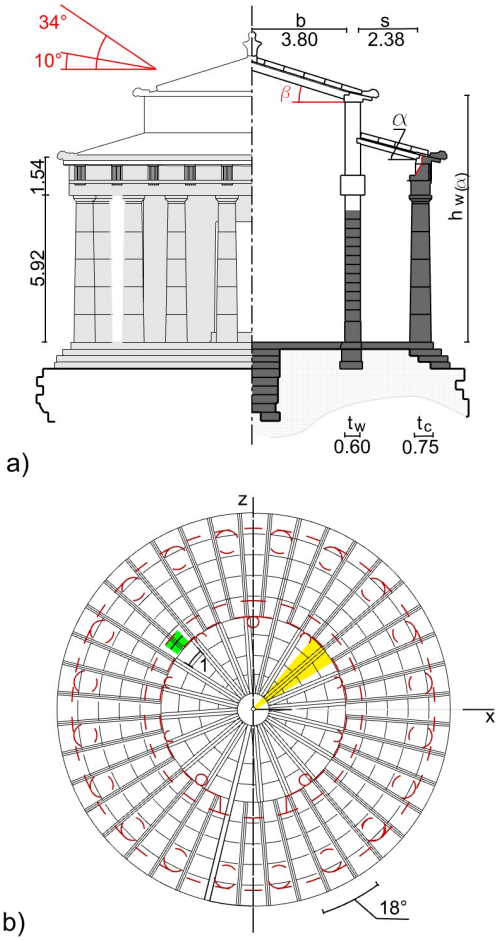


Figure 21 The double roof proposed by Pomtow, composed by two sets of rafters spanning respectively the cella and the peristyle. Plan view (a); elevation and possible section (b).

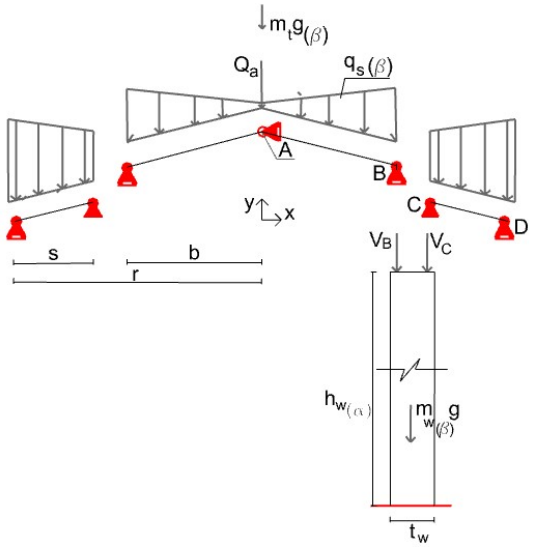


Figure 22 Structural diagrams of the double roof and the wall of the cella.

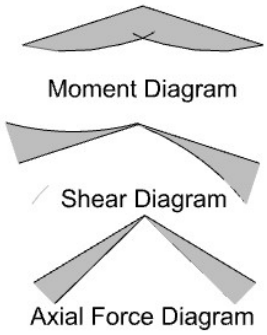


Figure 23 Typical diagrams of the internal forces and moment.

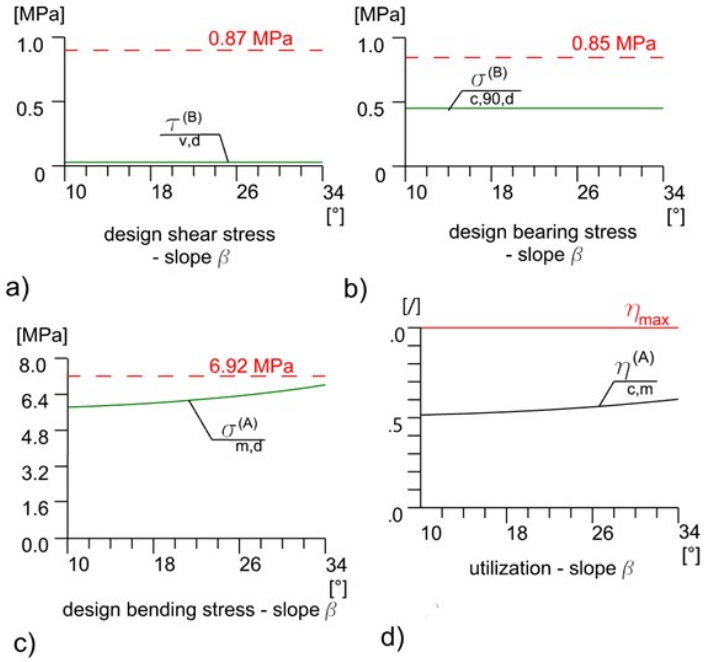


Figure 24 Structural analyses of one of the rafters covering the cella, for variable slope angle of the roof of the cella. Design shear stress (a); design bearing stress (b); design bending stress (c); utilization due to composed bending action and compression parallel to the fibers (d). The stress values are plotted alongside the limit values derived in Section 2.

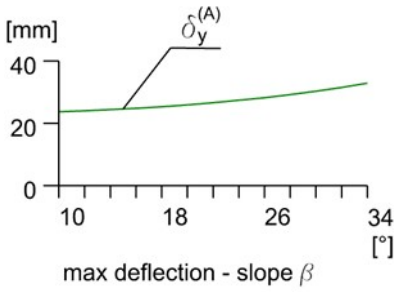


Figure 25 Maximum vertical deflection of the rafter spanning the cella, for variable slope of the roof.

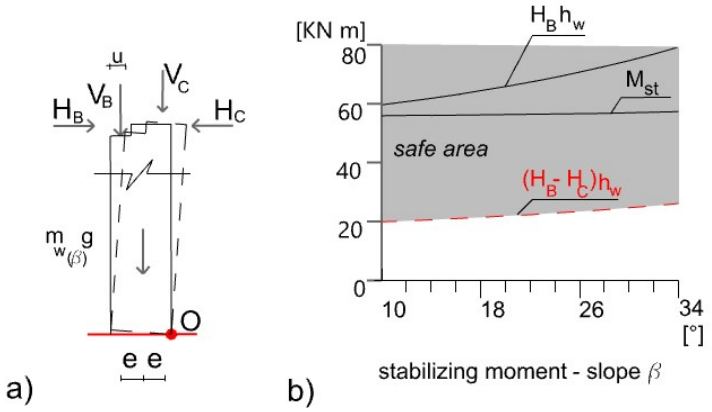


Figure 26 Free body diagram of a portion of the wall.(a). Stabilizing moment, Mst, plotted against the overturning moments exerted by the solo internal rafter and by the combination of external and internal ones.

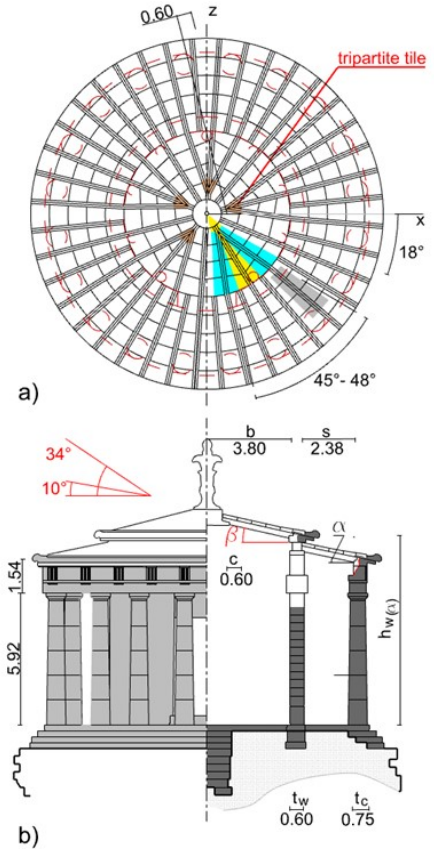


Figure 27 The double roof proposed by Hoepfner, where the cella is composed of standard and interconnecting rafters. Plan view (a); possible elevation and section (b).

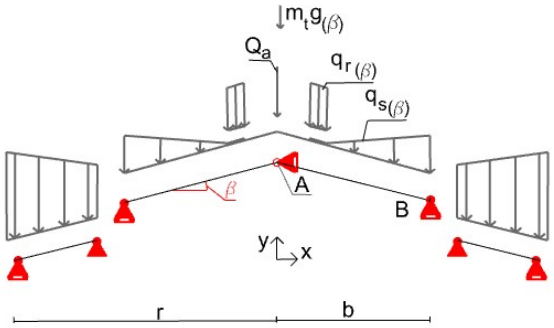


Figure 28 Structural diagram of the primary rafters. Notice the added load qr exerted by the ones resting on them.

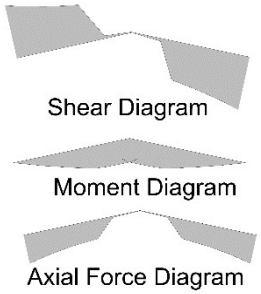


Figure 29 Typical force diagrams of the primary rafter. The load transmitted by the secondary rafters generates an abrupt increase of internal forces and moment.

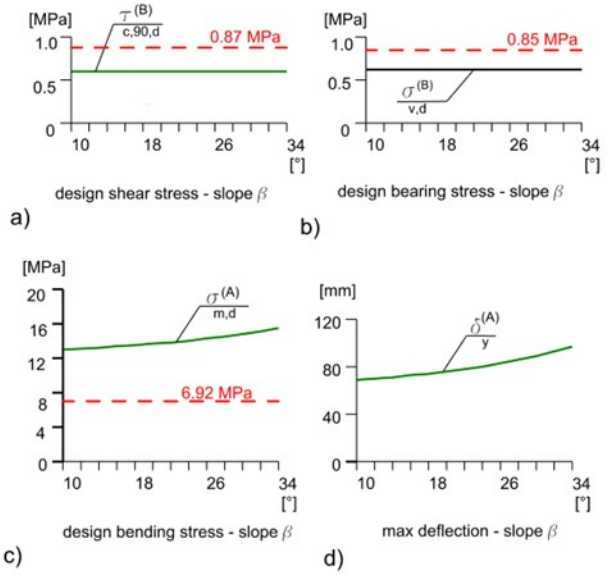


Figure 30 Structural analyses of the primary rafters covering the cella, for variable slope angle β of the roof of the cella. Design shear stress (a); design bearing stress at support (b); design bending stress (c); maximum vertical deflection (d). The stress values are plotted alongside the limit values derived in Section 2.

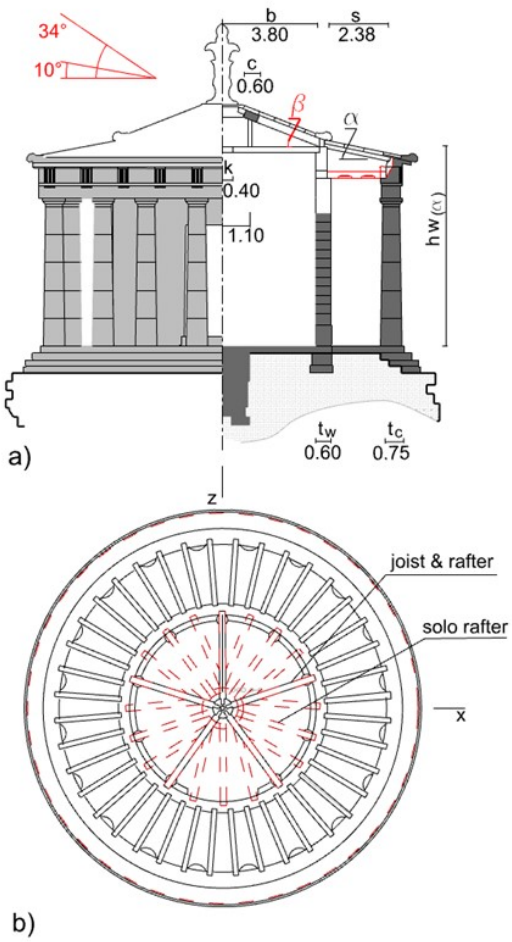


Figure 31 The double roof, composed by rafters and joists. Possible elevation and section (a); plan view (b).

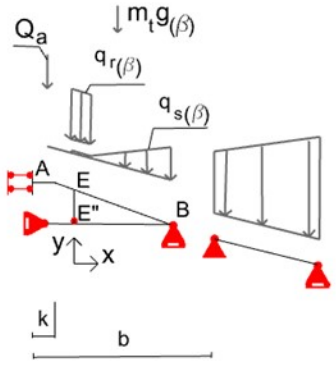


Figure 32 Structural diagram of one of the five systems of rafters, joists, and hangers.

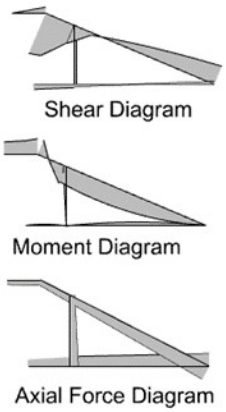


Figure 33 Typical force diagrams, plotted for variable slope angle β. It should be observed that, with increasing slope, the axial force in the prop changes from compression to tension.

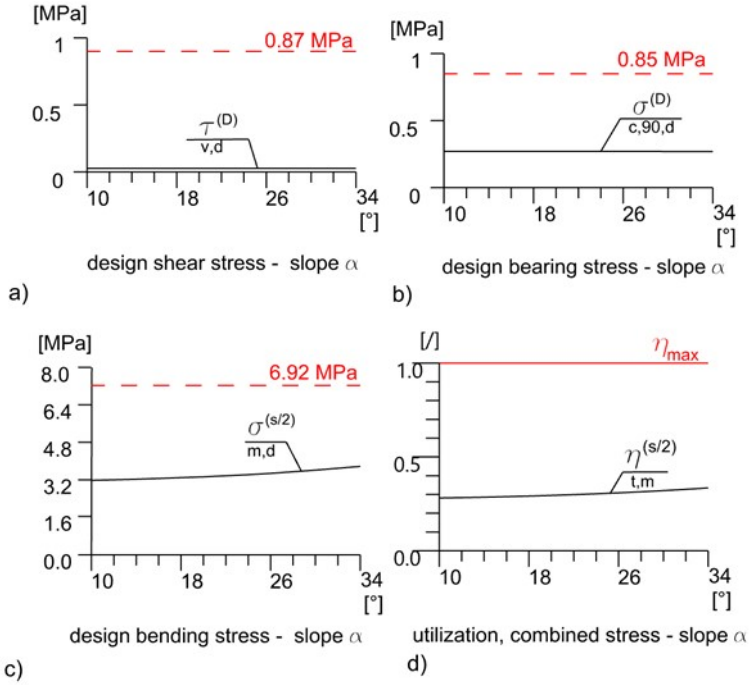


Figure 34 Strength analyses of the rafter and joist system, for variable slope angle of the roof of the cella. Design shear stress (a); design bearing stress at support (b); design bending stress (c); and maximum utilization (d). The stress values are plotted alongside the maximum values derived in Section 2.

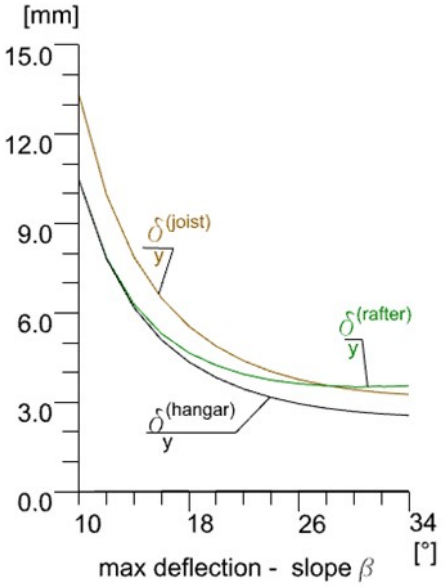


Figure 35 Maximum deflection on the elements composing the post and lintel structure as a function of the slope of the roof.